The second messenger c-di-AMP controls natural competence via ComFB signaling protein

Sherihan Samir[1,4,§], Sofía Doello[1,§], Erik Zimmer[1], Michael Haffner[1], Andreas M. Enkerlin[2], Teresa Müller[1], Lisa Dengler[1], Stilianos P. Lambidis[1], Shamphavi Sivabalasarma[3,5], Sonja-Verena Albers[3,6], Khaled A. Selim[1,2,6,*]

[1] Interfaculty Institute of Microbiology and Infection Medicine, Organismic Interactions Department, Cluster of Excellence "Controlling Microbes to Fight Infections", Tübingen University, 72076 Tübingen, Germany
[2] Microbiology/ Molecular Physiology of Prokaryotes, Institute of Biology, University of Freiburg, Schänzlestraße 1, 79104 Freiburg, Germany
[3] Molecular Biology of Archaea, Institute of Biology, University of Freiburg, Freiburg, Germany
[4] Microbiology Department, Faculty of Science, Ain Shams University, Cairo, Egypt
[5] Spemann Graduate School of Biology and Medicine, University of Freiburg, 79104 Freiburg, Germany
[6] Signalling Research Centres BIOSS and/or CIBBS, Faculty of Biology, Freiburg University, Freiburg, Germany
[§] These authors contributed equally to this work
*** Correspondence: Khaled A. Selim (khaled.selim@biologie.uni-freiburg.de)**

Natural competence requires a contractile pilus system. Here, we provide evidence that the pilus biogenesis and natural competence in cyanobacteria are regulated by the second messenger c-di-AMP. Furthermore, we show that the ComFB signaling protein is a novel c-di-AMP-receptor protein, widespread in bacterial phyla, and required for DNA uptake.

Second messengers are small molecules involved in regulating many processes in all kinds of organisms (Yoon & Waters 2021). Cyclic di-AMP is one of the recently discovered di-nucleotide-type second messengers only present in prokaryotes (Stülke & Krüger 2020; He et al. 2020; Yin et al. 2020; Mantovani et al. 2023a). Its functions have been mainly studied in firmicutes, where it plays an important role in osmo-adaptation by controlling potassium homeostasis and influencing transcription of genes related to osmosis and cell wall metabolism (Stülke & Krüger 2020; He et al. 2020; Yin et al. 2020; Herzberg et al. 2023; Nelson et al. 2013; Ren & Patel 2014). In cyanobacteria, c-di-AMP seems to control additional processes, including the diurnal metabolism via its binding to the carbon control protein SbtB to regulate glycogen metabolism (Rubin et al. 2018; Selim et al. 2021a). Although important roles for c-di-AMP have been acknowledged since its discovery, recent studies suggest broader regulatory impacts of c-di-AMP signaling with further functions yet to be elucidated (Mantovani et al. 2022; Haffner et al. 2023b). For instance, a role for c-di-AMP in controlling natural competence has been speculated in *Streptococcus pneumoniae*, although the molecular mechanism remained elusive (Zarrella et al. 2020). In this study, we aimed to investigate the involvement of c-di-AMP in natural competence.

Natural competence is a conserved mechanism of horizontal gene transfer that permits massive genetic variation and genomic plasticity via uptake of extracellular DNA, and it is the main cause of spreading antibiotic resistance and acquisition of virulence factors (Gibson & Venning 2023; Ellison et al. 2018).

This process involves a contractile pilus system and an assemblage of competence-accessory proteins (Taton et al. 2020; Ellison et al. 2018; Chen et al. 2020). In cyanobacteria, natural competence is under circadian clock control, with pili biogenesis occurring during the day phase and competence being induced with the onset of the night, when the circadian peaks (Taton et al. 2020). In the cyanobacterium *Synechocystis* sp. PCC 6803, the cellular levels of c-di-AMP and the transcription of its synthesizing di-adenylate cyclase gene (*dacA*), also follow a circadian rhythm: They decline during the night and increase sharply at the onset of the day (Selim et al. 2021a).

To test the involvement of c-di-AMP in natural competence, we compared the ability of the wildtype (WT) *Synechocystis* strain and the c-di-AMP-free Δ*dacA* mutant to take up DNA. Both strains were incubated with various extracellular DNA constructs containing a sequence that allows the insertion of a chloramphenicol resistance cassette via homologous recombination in a neutral site in the genome. The transformation efficiency for each strain was determined by analyzing the ability of these cells to grow on agar plates in the presence of chloramphenicol. The Δ*dacA* mutant showed significantly lower transformation efficiency than the WT, implying an essential role of c-di-AMP in natural competence (Figs. 1A and S1). Introducing a plasmid containing the *dacA* gene under the control of the P*petE* promoter into the Δ*dacA* strain restored the transformation efficiency to WT levels. Introducing the same plasmid into the WT to generate a c-di-AMP overexpression strain (WT::petE-*dacA*) did not affect the transformation efficiency. These results indicate that the absence of c-di-AMP affects cyanobacterial natural competence negatively, whereas high c-di-AMP does not. A similar result (Fig. S1) was obtained using the c-di-AMP-null Δ*cdaA* mutant of *Synechococcus elongatus* (Rubin et al. 2018), indicating that the c-di-AMP–dependent control of natural competence is a common trait among cyanobacteria.

To gain insights into the molecular basis of c-di-AMP-dependent control of natural competence, we checked how the lack of this second messenger affects pilus biogenesis. Proteome analysis of the Δ*dacA* mutant compared to WT cells under day-night cycle, a condition triggering pili biogenesis and natural competence (Taton et al. 2020), revealed a strong downregulation of specific proteins involved in pilus biogenesis and DNA uptake in the Δ*dacA* mutant (Haffner et al. 2023b). These changes were marked by a reduced abundance of PilT1 (Slr0161), PilM (Slr1274), PilN (Slr1275), PilO (Slr1276), and Sll0180 proteins (Table S1). The levels of the other pilus machinery proteins, including the extracellular pilin PilA1, were not significantly altered in the Δ*dacA* mutant (Table S1). The assembly of a functional pilus requires two motor ATPases, PilB1 and PilT1. PilT1 is located at the pilus base and is required for retraction and depolymerization. Therefore, the *pilT1* mutant is nonmotile, hyperpiliated and loses natural competence (Cengic et al. 2018; Bhaya et al. 2000; Okamoto & Ohmori 2002). The PilMNO proteins form the alignment complex, connecting the components of the pilus machinery in the inner and outer membranes by forming a ring-structure in the periplasm (Chang et al. 2016; Conradi et al. 2020; Chen et al. 2020). Similarly, the *pilM*, *pilN* and *pilO* mutants are nonmotile and non-transformable (Yoshihara et al. 2001). Sll0180 is an accessory protein of TolC-system, needed for the glycosylation

of PilA1 and the secretion of the S-layer protein, and thereby the correct assembly of the pilus machinery (Gonçalves et al. 2018). The absence of functional PilA1 causes a non-transformable phenotype (Yoshihara et al. 2001). Notably, our transcriptome analysis showed a partial downregulation of *pilT1* and *sll0180*, while the *pilT2* gene (*sll1533*; Bhaya et al. 2000) was strongly downregulated in Δ*dacA* (Table S2; Mantovani et al. 2022). These findings explain why Δ*dacA* cells lost their natural competence.

The striking decrease of PilT1 levels in Δ*dacA* suggested a strong defect in pilus assembly and retraction. To confirm this assumption, we examined negatively stained Δ*dacA* and WT cells by transmission electron microscopy (TEM). While we could detect both thick and thin pili in the WT, only thick pili were obvious in Δ*dacA* cells (Fig. S2). Additionally, Δ*dacA* mutant showed a hyperpiliation phenotype in analogy to *pilT1* mutant (Cengic et al. 2018; Bhaya et al. 2000; Okamoto & Ohmori 2002). In addition, quantification of the major pilin PilA1 in the exoproteome of the Δ*dacA* mutant via immunodetection revealed an accumulation of PilA1 compared to the WT cells (Fig. 1B), consistent with the hyperpiliation phenotype of Δ*dacA* cells. These findings clearly support the notion of a c-di-AMP-dependent control of pilus biogenesis and natural competence with dysregulation of various components of pilus machinery in Δ*dacA* cells.

The lack of nonretractable pili explains the inability of the Δ*dacA* strain to take up DNA. Interestingly, the downregulation of the above-mentioned proteins was not detected in the Δ*sbtB* mutant, which lacks the only known cyanobacterial c-di-AMP receptor (Table S3) (Selim et al. 2021a; Haffner et al. 2023b). Additionally, Δ*sbtB* behaved like the WT in our natural competence assays (Figs. 1A and S1). These data suggested the involvement of an additional, yet unknown, c-di-AMP receptor, required for natural competence. To identify this new c-di-AMP receptor, cell extracts of *Synechocystis* cells grown under day-night cycles were incubated with immobilized c-di-AMP and bound proteins were identified by mass spectrometry (Figs. 1C and S3). The identification of several known c-di-AMP targets: SbtB, as well as the transporters TrkA, KrtA, MthK, MgtE and NhaS5, validated our pulldowns (Selim et al. 2021a). Additionally, the Slr1970 protein was also enriched under both conditions. This protein possesses the competence factor B domain (domain PF10719 in the Pfam database) (Mistry et al. 2021) and therefore was annotated as ComFB in the NCBI's RefSeq database (Haft et al. 2023). Enrichment of ComFB correlated with the intracellular levels of c-di-AMP, where ComFB was 8 times more abundant in the day than in the night pulldown. This indicates that the abundance of ComFB follows the same pattern as the c-di-AMP synthesis with an increase during the day and a decrease at night (Selim et al. 2021a). ComFB is widespread among different bacterial phyla (Figs. 1D and S4), implying a fundamental role in cell physiology. In *Bacillus, comFB* forms an operon with *comFA* and *comFC*, which are known to be involved in DNA uptake (Sysoeva et al. 2015; Hahn et al 2019). In *Synechocystis* and other cyanobacteria, *comFB* forms an operon with *hfq,* which is also involved in DNA uptake and

motility (Fig. S5) (Dienst et al. 2008; Schuergers et al. 2014; Oeser et al. 2021; Conradi et al. 2020), strongly suggesting a potential function of ComFB in natural competence.

To validate ComFB as a novel c-di-AMP-binding protein, we used several biophysical methods after purifying recombinant His_8-ComFB protein. Size exclusion chromatography coupled to multiangle light scattering (SEC-MALS) showed a species of ~ 40.5 kDa (Fig. S6), indicating that the 20.4 kDa ComFB protein is dimer in solution. Using isothermal titration calorimetry (ITC), we measured the binding affinity of ComFB to c-di-AMP. The c-di-AMP binds exothermically to ComFB with high affinity in the low micromolar range of a $K_D \sim 2.6 \pm 0.11$ µM (Figs. 1E and S6), indicating that ComFB binds c-di-AMP specifically. This result was confirmed using nano differential scanning fluorimetry (nanoDSF) and thermal shift assays (Figs. S7 and S8), where c-di-AMP thermally stabilized ComFB significantly in a concentration-dependent manner. Moreover, we performed DRaCALA assays (Roelofs et al. 2011) using radiolabeled [^{32}P]c-di-AMP to test further the specificity of c-di-AMP-binding to ComFB in competition with various unlabeled nucleotides. DRaCALA titration assays revealed strong binding of [^{32}P]c-di-AMP to ComFB with a K_D value of 3.6 ± 5.4 µM (Fig. 1F), comparable to that obtained by ITC. In the competition assays, the unlabeled c-di-AMP competed with [^{32}P]c-di-AMP for binding to ComFB, but that was not the case for ATP, ADP, and cAMP, confirming that c-di-AMP binding to ComFB is specific. However, this assay revealed that ComFB could additionally bind c-di-GMP, as c-di-GMP efficiently competed with [^{32}P]c-di-AMP (Fig. 1G). Remarkably, a recent study showed that the ComFB homolog in the multicellular cyanobacterium *Nostoc*, named CdgR, controls cell size by binding c-di-GMP (Zeng et al. 2023). In fact, the filamentous cyanobacterium *Nostoc* sp. PCC7120 is regarded as being not naturally competent (Schirmacher et al. 2020), implying that ComFB or CdgR might play different roles in multicellularity lifestyle.

To ascertain whether c-di-AMP binding to CdgR is of physiological relevance, we performed a pulldown assay with immobilized c-di-AMP as described above but using cell extracts from *Nostoc* (Fig. S3). Indeed, we identified the ComFB homolog (CdgR; Alr3277) as one of the enriched proteins along with other known c-di-AMP receptor proteins. This result further confirms that both ComFB and CdgR specifically bind both cyclic di-nucleotides in both organisms. The existence of a crosstalk between c-di-AMP and c-di-GMP on ComFB awaits, however, further investigation. Crosstalk between second messenger nucleotides is perhaps a more common phenomenon than so far realized. Recently, it was found that the second messengers c-di-GMP and (p)ppGpp reciprocally control *Caulobacter crescentus* growth by competitive binding to a metabolic switch protein, SmbA (Shyp et al. 2021). SbtB plays a similar role in cyanobacterial physiology and binds both cAMP and c-di-AMP (Selim et al. 2018, 2021a, 2023; Forchhammer et al. 2022). Likewise, the mycobacterial transcription factor DarR, which is regulated by c-di-AMP-binding, was found to be regulated as well through cAMP-binding (Schumacher et al. 2023). Additionally, crosstalk between cyclic guanosine and adenosine second messengers is also known, as the CRP-Fnr transcription factors are known to bind both cAMP and

cGMP, being only active in the cAMP-bound form in *E. coli*, while both cyclic nucleotides mediate the CRP activation in *Sinorhizobium meliloti* (Krol et al. 2023; Werel et al. 2023). Furthermore, both of cAMP and cGMP were found also to bind and modulate the activity of the AphA phosphatase in *E. coli* and *Haemophilus influenzae* (Kronborg & Zhang 2023).

To clarify if ComFB plays a role in natural competence, we created a Δ*slr1970* deletion mutant (Δ*comFB*; Fig. S9) and tested its natural competence ability by taking up DNA as described above (Fig. 1H). Like Δ*dacA,* Δ*comFB* showed reduced transformation efficiency as compared to the WT and Δ*sbtB* cells. Complementation of Δ*comFB* mutant with *comFB* gene under a P*petE* promoter restored the WT competence phenotype (Fig. 1H). Interestingly, no impairment in DNA uptake was observed for Δ*sbtB,* which lacks another c-di-AMP receptor protein and showed a similar transformation rate to the WT (Figs. S1). These findings further support that natural competence depends on c-di-AMP signaling and is controlled specifically by a pathway that involves ComFB as a c-di-AMP receptor protein, while other c-di-AMP targets are not involved in this process. Notably, in contrast to Δ*sbtB* (Selim et al. 2021a), the Δ*comFB* mutant did not show any impairment under diurnal growth or prolonged dark incubation (Fig. S10), supporting the notion that c-di-AMP plays different signaling functions through binding to different cellular receptors.

To rule out that the transformation deficiency observed in Δ*dacA* mutant (Fig. 1A) is due to a downstream effect on the intracellular c-di-GMP content, which is known to regulate motility-related functions (Mantovani et al. 2023a; Enomoto et al. 2023), we measured the c-di-GMP levels in Δ*dacA* during the day and the night phases (Fig. S11). The c-di-GMP levels were comparable in both strains within the light/dark phases, thus confirming that DNA uptake is influenced by c-di-AMP specifically.

In conclusion, our results show that the regulation of pili biogenesis and natural competence is a new unexplored role of c-di-AMP, which requires the receptor protein ComFB. In a broader context, natural competence is a primary mode of horizontal gene transfer, which plays an important role in spreading multidrug resistance. It would therefore be highly interesting to determine whether the influence of c-di-AMP and ComFB signaling in DNA uptake extends to other bacteria, especially those of clinical relevance. Collectively, we identified ComFB as a novel widespread c-di-NMP-receptor protein, which turned out to be a pivotal competence-accessory protein, at least in cyanobacteria, likely regulating the pili biogenesis at transcriptional level by an as-yet unknown mechanism.

Materials and Methods

Protein production and purification: All the plasmids and primers used in this study are listed in (Table S4). The *slr1970* (encoding ComFB) and *slr1513* (encoding SbtB) from *Synechocystis* sp. PCC 6803 were cloned into the pET-28a vector with Gibson assembly, thereby incorporating a C-terminal His_8-tag. Positive clones were selected on 50 µg/mL kanamycin agar plates. The expression and purifications of His_8-ComFB, His_6-DisA and His_8-SbtB proteins were achieved as described previously (Selim et al. 2019, 2021b). The proteins were

recombinantly produced in *E. coli* strain LEMO21 (DE3) by overnight induction at 20 °C using 0.5 mM IPTG. Cells were lysed by sonication and the soluble proteins (ComFB, DisA or SbtB) were purified by immobilized metal affinity chromatography (IMAC) using Ni^{2+}-Sepharose resin (cytiva^{TM}), followed by size exclusion chromatography (SEC) using a Superdex 200 Increase 10/300 GL column (GE HealthCare). Protein purity was assessed by Coomassie-stained SDS-PAGE, and protein concentrations were determined using Bradford assay. Analytical SEC coupled to multi-angle light scattering (SEC-MALS) was conducted as described previously to calculate the molar mass of ComFB protein, whereas SbtB was used as a control (Selim et al. 2019, 2020; Walter et al. 2019).

Synthesis of [^{32}P]c-di-AMP: The pGP2563 plasmid (pET19b-based; kindly provided by Jörg Stülke), expressing an active di-adenylate cyclase His_6-DisA from *Bacillus subtilis* (Mehne et al. 2013), was used to express and purify DisA. Twenty µM or 50 µM DisA were incubated in DisA reaction buffer (40 mM Tris/HCl [pH 7.5], 100 mM NaCl and 10 mM $MgCl_2$) with 1 mM ATP at 30 °C overnight with 300 rpm shaking. Samples were centrifuged for 10 min at 14.000 rpm to remove precipitated protein. Then, the supernatant was filtered through Amicon® Ultra – 0.5 mL 10-kDa cutoff centrifugal filters (Merck KgaA; Darmstadt, Germany). To test the enzymatic efficiency of DisA before synthesizing [^{32}P]c-di-AMP, DisA was incubated with unlabeled ATP and 15 µl of the reaction product was analysed by thin layer chromatography (TLC; POLYGRAM CEL300 PEI plates) (Macherey-Nagel GmbH & Co. KG, Düren, Germany) using a running buffer of [1 vol. Saturated NH_4SO_4 (4.2 M) and 1.5 volumes 1.5 M KH_2PO_4 (pH 3.6)] (Fig. S12). Via injecting 5 µl of the reaction product, the activity of DisA was further confirmed by LC-MS (ESI-TOF mass spectrometer; MicrO-TOF II, Bruker) connected to Ultimate 3000 HPLC system (Dionex) on C18 column (Phenomenex, 150×4.6 mm, 110 Å, 5 µm) and using a flow rate of 0.2 mL/min and a 45 min program (for 5 min, 100 % buffer A (0.1 % formic acid with 0.05% ammonium formate), then 30 min of a linear gradient to 40 % buffer B (100 % acetonitrile), and 10 min of column re-equilibration with 100 % buffer A). Data are presented as extracted ion chromatograms (EICs) for ATP and c-di-AMP (Fig. S12). Finally, 250 µCi radiolabeled [^{32}P]c-di-AMP was synthesized from [α-^{32}P]ATP (6000 mCi/µmol) by using His_6-tagged DisA by Hartmann Analytic GmbH (Braunschweig, Germany).

***In vitro* protein-ligand binding assays:** Binding of recombinantly produced ComFB to c-di-AMP was analysed *in vitro* by isothermal titration calorimetry (ITC), thermal shift assay (TSA), and differential scanning fluorimetry (nanoDSF), as described previously (Lapina et al. 2018; Haffner et al. 2023a; Mantovani et al. 2023b). For ITC and TSA, both ComFB and c-di-AMP were dissolved in binding buffer (50 mM Tris/HCl, pH 8.0, 300 mM NaCl, 0.55 mM EDTA). ITC measurements were conducted on a MicroCal PEAQ-ITC instrument (Malvern Panalytical), at 25 °C, with a reference power of 10 µcal/s. Different ComFB protein concentrations in the range of 60-172 µM were titrated against 0.5 or 1 mM c-di-AMP. A control experiment was recorded by titration of c-di-AMP over a cell filled with buffer, to measure the dilution heat of c-di-AMP. Data were analyzed using one set of binding sites model with the MicroCal PEAQ-ITC Analysis Software (Malvern Panalytical) to calculate the dissociation constant K_D. The dilution heat of the control ITC buffer/c-di-AMP experiments were subtracted from the ComFB/c-di-AMP runs. For reproducibility, different patches of ComFB protein purifications were used in different ITC experiments. TSA measurements were conducted on an iQ5 Real-Time PCR detection system (Bio-Rad). ComFB (10-39 µM) and 0-1.2 mM c-di-AMP were mixed in different ratios, with the addition of 10x SYPRO Orange. All conditions were measured in triplicate in sealed 96-well plates by following the dye's

fluorescence emission over a temperature range of 25 to 99 °C. Data were analysed with OriginPro software (OriginLab Corporation) and Python. For nanoDSF (Nanotemper), both ComFB and SbtB proteins were diluted in the ITC buffer and used at 1.5 mg/mL concentration with or without 0.5 mM c-di-AMP. The proteins autofluorescence (350/330 nm ratio), as well as light scattering were measured in a temperature range of 30-99 °C to determine the melting curve and the rate of protein unfolding.

Differential Radial Capillary Action of Ligand Assay (DRaCALA): The specificity of c-di-AMP binding to ComFB has been verified using DRaCALA (Differential Radial Capillary Action of Ligand Assay) (Roelofs et al. in 2011) using either *E. coli* cell lysate or purified proteins. For cell lysate, ComFB or SbtB has been overexpressed in *E. coli* LEMO21 (DE3), and cell lysates were used for the DRaCALA assays. In the DRaCALA assays, the cell lysates (with total protein concentration of 20 µg) or purified proteins (ComFB or SbtB) were mixed with 2 nM of a radioactively labeled [^{32}P]c-di-AMP (~ 6000 mCi/µmol) for 15 min at room temperature in a binding buffer of (10 mM Tris/HCl [pH 8.0], 100 mM NaCl and 5 mM $MgCl_2$). In the competition binding assays, the [^{32}P]c-di-AMP was incubated first for 2 mins with the protein or the cell lysates, before adding 1 mM of unlabeled nucleotides (c-di-AMP, c-di-GMP, ATP, ADP, and cAMP) to the reaction mixture for 15 mins. Finally, 10 µL of each mixture were dropped on a nitrocellulose membrane (Amersham™ ProtanTM 0.2 µm NC, Catalogue No10600001, Cytiva Europe GmbH, Freiburg), which binds to the protein while the free ligands diffuse, thereby a radioactive signal appears at the center of the drop application in case of binding of the [^{32}P]c-di-AMP to ComFB. After drying, the nitrocellulose membranes were transferred into an X-ray film cassette and the imaging plates (BAS-IP MS 2025, 20 x 25 cm, FUJIFILM Europe GmbH, Düsseldorf, Germany) were placed directly onto the nitrocellulose membrane, then the cassettes were closed and incubated overnight. The next day, the plates were imaged with a Typhoon™ FLA9500 PhosphorImager (GE Healthcare). For [^{32}P]c-di-AMP signal quantification, the image analysis software Image Studio Lite Ver 5.2.5 was used. The fraction of bound nucleotide was calculated based on (Roelofs et al. 2011) using the following equation:

$$F_B = \frac{I_{inner} - \left[A_{inner} \times \frac{(I_{total} - I_{inner}}{(A_{total} - A_{inner}\right]}}{I_{total}}$$

In the DRaCALA competition assays, if one of the unlabeled nucleotides binds to the ComFB, it will compete on the same binding sites and will reduce or eradicate the radioactive signal of [^{32}P]c-di-AMP binding to ComFB. SbtB, a known c-di-AMP receptor protein (Selim et al. 2021a), and extract of *E. coli* cells expressing an empty plasmid were used as positive and negative controls, respectively.

Phylogenetic analysis: Phylogenetic analysis was done essentially as described elsewhere (Neumann et al. 2022). Homologous protein sequences to the ComFB full-length protein (Slr1970, amino acids 1-173) and to the ComFB-domain only (amino acids 57-147) were searched against the Ref-Seq Select proteins database, using the NCBI blastp suite. ComFB hits were filtered (expectation value $E \leq 10^{-3}$). The sequences were submitted to multiple sequence alignments (MSA) using COBALT (NCBI). Phylogenetic trees were constructed based on the MSAs and visualized using the iTOL online tool (Letunic et al. 2021).

Construction of mutant strains: The unicellular, freshwater cyanobacterium *Synechocystis* sp. PCC 6803, described in (Selim et al. 2021a), was used as the reference wildtype strain in this study. All plasmids and primers used in this study are listed in (Table S4). All constructs used in this study were generated using Gibson assembly.

All knockout mutants were generated with homolog recombination using the natural competence of *Synechocystis* sp. PCC 6803, as described previously (Selim et al. 2018).

For generation of knockout deletion mutants, the mutants were constructed by deleting the ORFs *slr1513*, *sll0505*, and *slr1970* (designated *sbtB*, *dacA*, and *comFB*, respectively) and replaced with the erythromycin, kanamycin, and spectinomycin resistance cassette, respectively. The Δ*sbtB* and Δ*dacA* knockout mutants were created, as described previously (Selim et al. 2018, 2021a). For generation of the knockout mutation in the *slr1970* ORF (designated *comFB*; Fig. S9), a synthetic DNA fragment encoding the upstream and downstream regions of *slr1970* (0.5 kb) and the spectinomycin resistant cassette (gBlock, IDT, USA) were cloned into digested pUC19 vector using the Gibson cloning strategy. For complementation, the Δ*dacA*::petE-*dacA*, WT::petE-*dacA* and Δ*comfB*::petE-*comfB* strains were generated by introducing the *dacA* gene (*sll0505*) or comfB gene (*slr1970*) under the control of Cu^{2+} inducible promoter P*petE* into respective mutant backgrounds using the self-replicating plasmid pVZ322, as described previously (Selim et al. 2018, 2021b).

The c-di-AMP-free mutant of *Synechococcus elongatus* PCC 7942 was created as described previously (Rubin et al. 2018) using a *cdaA*-deletion plasmid (AM5403; kindly gifted from Susan Golden) carrying the spectinomycin/streptomycin resistance gene *aadA*. All the plasmids used to generate the mutants were verified by sequencing and then transformed in *Synechocystis* sp. PCC6803, as described (Selim et al. 2018). All mutants were selected on BG_{11} plates supplemented with proper antibiotics and verified by PCR.

Transformation assay: Natural transformation competence was assessed with different suicide plasmids, all encoding chloramphenicol resistance and integrating into different places in the *Synechocystis* sp. PCC 6803 genome (Oeser et al. 2021). Briefly, the cells of wildtype (WT) *Synechocystis* or respective mutants (Δ*dacA*, Δ*sbtB*, Δ*comfB*, Δ*dacA*::petE-*dacA*, WT::petE-*dacA* and Δ*comfB*::petE-*comfB*) were cultivated in BG_{11} (50 mL) at 28 °C, constant 50 µE m^{-2} s^{-1} and shaking to an OD_{750} of 0.7, then harvested at 4,000 g for 20 min. Cell pellets were resuspended in 600 µl of BG_{11} and all samples were adjusted to the same OD_{750}. Cells suspensions were transferred to a 1.5 mL tube and 1 µg of different plasmids, containing chloramphenicol resistance cassette, were added to ensure the reproducibility. The 1.5 mL tubes were covered with aluminum foil and incubated at 28 °C for 3 h, then gently inverted and incubated for 3 more h. 0.45 µm HATF membranes (HATF08250, Sigma-Aldrich, Germany) were placed on BG_{11} plates and 200 µl of the cell suspensions were spread on them. Plates were incubated at 28 °C and 50 µE m^{-2} s^{-1} for 16 h and membranes were then transferred to BG_{11} plates supplemented with 15 µg/mL of chloramphenicol. After 48 h of incubation at 28 °C and 50 µE m^{-2} s^{-1}, membranes were transferred to BG_{11} plates supplemented with 30 µg/mL of chloramphenicol and further incubated until singles colonies were visible. At least three-five biological replicates were used for each strain. Some clones were verified by PCR for the insertion of chloramphenicol cassette into the genome. The natural transformation competence for WT *S. elongatus* and *cdaA* mutant was done as described for *Synechocystis* but using a plasmid carrying kanamycin resistance cassette.

Exoproteome analysis: *Synechocystis* sp. PCC 6803 wildtype and Δ*dacA* cells were grown in 250 mL of BG_{11} at 28 °C, constant 50 µE m^{-2} s^{-1} and shaking to an OD_{750} of 0.8. Cultures were spun down at 4,000 g for 20 min and the supernatant was filtered through cellulose nitrate membrane filters (7182-004, Cytiva, Marlborough, MA, USA) and concentrated to 1 mL using Amicon Ultra-15 centrifugal filters with a cutoff of 10 kDa (UFC901024, Sigma-Aldrich). Three biological replicates were prepared for each strain. Immunoblot detection

of PilA1 in the exoproteome extracts was done as previously described (Oeser et al. 2021) using α-PilA1 antibody (kindly provided by Roman Sobotka; Linhartová et al. 2014).

Transmission electron microscopy (TEM): Cells (WT, Δ*dacA* and WT::petE-*dacA*), growing BG_{11} at 28°C under continuous illumination 50 µE m^{-2} s^{-1}, were negatively stained with 2% aqueous uranyl acetate (w/v). Imaging was done with Hitachi HT7800 operated at 100 kV, equipped with an EMSIS Xarosa 20-megapixel CMOS camera (Oeser et al. 2021). Acquired images were analyzed with ImageJ.

Mass spectrometry-based proteomics analysis: The full proteomics analysis of the *Synechocystis* sp. PCC 6803 wildtype, Δ*sbtB* and Δ*dacA* cells, growing under day-night cycles, was done as described previously in (Haffner et al. 2023b). The full proteomics data sets are described in (Haffner et al. 2023b). The pulldown experiments to identify the potential c-di-AMP target proteins was done as described previously (Selim et al. 2021a) using *Synechocystis* sp. (under day and night conditions) and *Nostoc*. sp. PCC 7120 cell extracts. The determination of intracellular c-di-GMP concentration in wildtype and Δ*dacA* cells was done as described in (Selim et al. 2021a) using mass spectrometry calibrated with $^{13}C_{20}{}^{15}N_{10}$-c-di-GMP and $^{13}C_{20}{}^{15}N_{10}$-c-di-AMP (200 ng/ml each).

Data availability: The mass spectrometry proteomics data have been deposited to the ProteomeXchange Consortium via the PRIDE partner repository with the dataset identifier PXD045008.

Acknowledgements

The project was funded by grants from the German Research Foundation (DFG) as part of the priority research programs (SPP1879) and (SPP2389; SE 3449/1-1) to KAS and MH, and by the collaborative research center SFB1381 (project number: 403222702) to KAS, SAV and SSiv. KAS gratefully acknowledges Karl Forchhammer for continued support, and acknowledges the infrastructural support by the Cluster of Excellence "Controlling Microbes to Fight Infections (CMFI)" (EXC2124–390838134) and by the Excellence Strategy of the German Federal and Baden-Württemberg State Governments (Projektförderung: PRO-SELIM-2022-14). We would like to thank Jörg Stülke (Göttingen University), Annegret Wilde (Freiburg University), Michael Galperin (NCBI), Susan Golden (University of California San Diego) and Roman Sobotka (South Bohemia University) for valuable comments and/or sharing materials with us, and the staff of the isotope laboratory and the proteome center (Tübingen University) for their excellent support. We would like to thank also the EM facility at the Faculty of Biology, University of Freiburg, for access to the TEM. The TEM (Hitachi HT7800) was funded by the DFG grant (project number: 426849454) and is operated by University of Freiburg (Faculty of Biology) as a partner unit within the Microscopy and Image Analysis Platform (MIAP) and the Life Imaging Center (LIC). We are also grateful to Heinz Grenzendorf, Markus Burkhardt, Filipp Oesterhelt and Marina Borisova (Tübingen University), and Reinhard Albrecht (MPI for Biology Tübingen) for the excellent support and/or assistance.

Author contributions

KAS conceived, initiated, designed and supervised the research; SSam, SD, EZ, MH, LD, TM, SPL, SSiv and KAS performed research; SVA supervised the TEM analysis; SSam, SD, EZ, and KAS analyzed data and prepared the figures; and SD and KAS wrote the manuscript. All authors approved the final version of the manuscript.

Competing interests

The authors declare no competing interest.

References

1. Bhaya D, Bianco NR, Bryant D, Grossman A. Type IV pilus biogenesis and motility in the cyanobacterium Synechocystis sp. PCC6803. Mol Microbiol. 2000; 37(4):941-51. doi: 10.1046/j.1365-2958.2000.02068.x.
2. Carbon signaling protein SbtB possesses atypical redox-regulated apyrase activity to facilitate regulation of bicarbonate transporter SbtA. Proc Natl Acad Sci USA. 2023; 120(8):e2205882120. doi: 10.1073/pnas.2205882120.
3. Cengic I, Uhlén M, Hudson EP. Surface Display of Small Affinity Proteins on Synechocystis sp. Strain PCC 6803 Mediated by Fusion to the Major Type IV Pilin PilA1. J Bacteriol. 2018; 200(16):e00270-18. doi: 10.1128/JB.00270-18.
4. Chang YW, Rettberg LA, Treuner-Lange A, Iwasa J, Søgaard-Andersen L, Jensen GJ. Architecture of the type IVa pilus machine. Science. 2016 Mar 11;351(6278):aad2001. doi: 10.1126/science.aad2001. Epub 2016 Mar 10. Erratum in: Science. 2016; 352(6282). pii: aaf7977. doi: 10.1126/science.aaf7977.
5. Chen Z, Li X, Tan X, Zhang Y, Wang B. Recent Advances in Biological Functions of Thick Pili in the Cyanobacterium *Synechocystis* sp. PCC 6803. Front Plant Sci. 2020; 11:241. doi: 10.3389/fpls.2020.00241.
6. Conradi FD, Mullineaux CW, Wilde A. The Role of the Cyanobacterial Type IV Pilus Machinery in Finding and Maintaining a Favourable Environment. Life (Basel). 2020; 10(11):252. doi: 10.3390/life10110252.
7. Dienst D, Dühring U, Mollenkopf HJ, Vogel J, Golecki J, Hess WR, Wilde A. The cyanobacterial homologue of the RNA chaperone Hfq is essential for motility of Synechocystis sp. PCC 6803. Microbiology (Reading). 2008; 154(Pt 10):3134-3143. doi: 10.1099/mic.0.2008/020222-0.
8. Ellison CK, Dalia TN, Vidal Ceballos A, Wang JC, Biais N, Brun YV, Dalia AB. Retraction of DNA-bound type IV competence pili initiates DNA uptake during natural transformation in Vibrio cholerae. Nat Microbiol. 2018; 3(7):773-780. doi: 10.1038/s41564-018-0174-y.
9. Enomoto G, Wallner T, Wilde A. Control of light-dependent behaviour in cyanobacteria by the second messenger cyclic di-GMP. Microlife. 2023; 4:uqad019. doi: 10.1093/femsml/uqad019.
10. Forchhammer K, Selim KA, Huergo LF. New views on PII signaling: from nitrogen sensing to global metabolic control. Trends Microbiol. 2022; 30(8):722-735. doi: 10.1016/j.tim.2021.12.014.
11. Gibson PS, Veening JW. Gaps in the wall: understanding cell wall biology to tackle amoxicillin resistance in Streptococcus pneumoniae. Curr Opin Microbiol. 2023; 72:102261. doi: 10.1016/j.mib.2022.102261.
12. Gonçalves CF, Pacheco CC, Tamagnini P, Oliveira P. Identification of inner membrane translocase components of TolC-mediated secretion in the cyanobacterium Synechocystis sp. PCC 6803. Environ Microbiol. 2018; 20(7):2354-2369. doi: 10.1111/1462-2920.14095.
13. Haffner M, Hou W-T, Mantovani O, Walke PR, Hauf K, Borisova M, Hagemann M, Zhou C-Z, Forchhammer K, Selim KA. PII signal transduction superfamily acts as a valve plug to control bicarbonate and ammonia homeostasis among different bacterial phyla. BioRxiv 2023a; doi: https://doi.org/10.1101/2023.08.10.552651
14. Haffner M, Mantovani O, Spät P, Maček B, Hagemann M, Forchhammer K, Selim KA. Diurnal rhythm causes metabolic crises in the cyanobacterial mutants of c-di-AMP signalling cascade. BioRxiv 2023b; doi: https://doi.org/10.1101/2023.11.14.567006
15. Haft DH, Badretdin A, Coulouris G, DiCuccio M, Durkin AS, Jovenitti E, Li W, Mersha M, O'Neill KR, Virothaisakun J, Thibaud-Nissen F. RefSeq and the prokaryotic genome annotation pipeline in the age of metagenomes. Nucleic Acids Res. 2023; gkad988. doi: 10.1093/nar/gkad988.
16. Hahn J, DeSantis M, Dubnau D. Mechanisms of Transforming DNA Uptake to the Periplasm of Bacillus subtilis. mBio. 2021; 12(3):e0106121. doi: 10.1128/mBio.01061-21.
17. He J, Yin W, Galperin MY, Chou SH. Cyclic di-AMP, a second messenger of primary importance: tertiary structures and binding mechanisms. Nucleic Acids Res. 2020; 48(6):2807-2829. doi: 10.1093/nar/gkaa112.
18. Herzberg C, Meißner J, Warneke R, Stülke J. The many roles of cyclic di-AMP to control the physiology of *Bacillus subtilis*. Microlife. 2023; 4:uqad043. doi: 10.1093/femsml/uqad043.
19. Krol E, Werel L, Essen LO, Becker A. Structural and functional diversity of bacterial cyclic nucleotide perception by CRP proteins. Microlife. 2023; 4:uqad024. doi: 10.1093/femsml/uqad024.

20. Kronborg K, Zhang YE. cAMP competitively inhibits periplasmic phosphatases to coordinate nutritional growth with competence of *Haemophilus influenzae*. J Biol Chem. 2023; 105404. doi: https://doi.org/10.1016/j.jbc.2023.105404
21. Lapina T, Selim KA, Forchhammer K, Ermilova E. The PII signaling protein from red algae represents an evolutionary link between cyanobacterial and Chloroplastida PII proteins. Sci Rep. 2018; 8(1):790. doi: 10.1038/s41598-017-19046-7.
22. Letunic I, Bork P. Interactive Tree Of Life (iTOL) v5: an online tool for phylogenetic tree display and annotation. Nucleic Acids Res. 2021; 49(W1):W293-W296. doi: 10.1093/nar/gkab301.
23. Linhartová M, Bučinská L, Halada P, Ječmen T, Setlík J, Komenda J, Sobotka R. Accumulation of the Type IV prepilin triggers degradation of SecY and YidC and inhibits synthesis of Photosystem II proteins in the cyanobacterium Synechocystis PCC 6803. Mol Microbiol. 2014; 93(6):1207-23. doi: 10.1111/mmi.12730.
24. Mantovani O, Haffner M, Selim KA, Hagemann M, Forchhammer K. Roles of second messengers in the regulation of cyanobacterial physiology: the carbon-concentrating mechanism and beyond. Microlife. 2023a; 4:uqad008. doi: 10.1093/femsml/uqad008.
25. Mantovani O, Haffner M, Walke P, Elshereef AA, Wagner B, Petras D, Forchhammer K, Selim KA, Hagemann M. The redox-sensitive R-loop of the carbon control protein SbtB contributes to the regulation of the cyanobacterial CCM. Research Square 2023b; doi: https://doi.org/10.21203/rs.3.rs-3292191/v1
26. Mantovani O, Reimann V, Haffner M, Herrmann FP, Selim KA, Forchhammer K, Hess WR, Hagemann M. The impact of the cyanobacterial carbon-regulator protein SbtB and of the second messengers cAMP and c-di-AMP on CO_2 -dependent gene expression. New Phytol. 2022; 234(5):1801-1816. doi: 10.1111/nph.18094.
27. Mehne FM, Gunka K, Eilers H, Herzberg C, Kaever V, Stülke J. Cyclic di-AMP homeostasis in bacillus subtilis: both lack and high level accumulation of the nucleotide are detrimental for cell growth. J Biol Chem. 2013; 288(3):2004-17. doi: 10.1074/jbc.M112.395491.
28. Mistry J, Chuguransky S, Williams L, Qureshi M, Salazar GA, Sonnhammer ELL, Tosatto SCE, Paladin L, Raj S, Richardson LJ, Finn RD, Bateman A. Pfam: The protein families database in 2021. Nucleic Acids Res. 2021; 49(D1):D412-D419. doi: 10.1093/nar/gkaa913.
29. Nelson JW, Sudarsan N, Furukawa K, Weinberg Z, Wang JX, Breaker RR. Riboswitches in eubacteria sense the second messenger c-di-AMP. Nat Chem Biol. 2013; 9(12):834-9. doi: 10.1038/nchembio.1363.
30. Neumann N, Friz S, Forchhammer K. Glucose-1,6-Bisphosphate, a Key Metabolic Regulator, Is Synthesized by a Distinct Family of α-Phosphohexomutases Widely Distributed in Prokaryotes. mBio. 2022; 13(4):e0146922. doi: 10.1128/mbio.01469-22.
31. Oeser S, Wallner T, Schuergers N, Bučinská L, Sivabalasarma S, Bähre H, Albers SV, Wilde A. Minor pilins are involved in motility and natural competence in the cyanobacterium Synechocystis sp. PCC 6803. Mol Microbiol. 2021 Sep;116(3):743-765. doi: 10.1111/mmi.14768.
32. Okamoto S, Ohmori M. The cyanobacterial PilT protein responsible for cell motility and transformation hydrolyzes ATP. Plant Cell Physiol. 2002; 43(10):1127-36. doi: 10.1093/pcp/pcf128.
33. Ren A, Patel DJ. c-di-AMP binds the ydaO riboswitch in two pseudo-symmetry-related pockets. Nat Chem Biol. 2014; 10(9):780-6. doi: 10.1038/nchembio.1606.
34. Roelofs KG, Wang J, Sintim HO, Lee VT. Differential radial capillary action of ligand assay for high-throughput detection of protein-metabolite interactions. Proc Natl Acad Sci USA. 2011; 108(37):15528-33. doi: 10.1073/pnas.1018949108.
35. Rubin BE, Huynh TN, Welkie DG, Diamond S, Simkovsky R, Pierce EC, Taton A, Lowe LC, Lee JJ, Rifkin SA, Woodward JJ, Golden SS. High-throughput interaction screens illuminate the role of c-di-AMP in cyanobacterial nighttime survival. PLoS Genet. 2018; 14(4):e1007301. doi: 10.1371/journal.pgen.1007301.
36. Schirmacher AM, Hanamghar SS, Zedler JAZ. Function and Benefits of Natural Competence in Cyanobacteria: From Ecology to Targeted Manipulation. Life (Basel). 2020; 10(11):249. doi: 10.3390/life10110249.

37. Schuergers N, Ruppert U, Watanabe S, Nürnberg DJ, Lochnit G, Dienst D, Mullineaux CW, Wilde A. Binding of the RNA chaperone Hfq to the type IV pilus base is crucial for its function in Synechocystis sp. PCC 6803. Mol Microbiol. 2014 May;92(4):840-52. doi: 10.1111/mmi.12595.
38. Schumacher MA, Lent N, Chen VB, Salinas R. Structures of the DarR transcription regulator reveal unique modes of second messenger and DNA binding. Nat Commun. 2023; 14(1):7239. doi: 10.1038/s41467-023-42823-0.
39. Selim KA, Haase F, Hartmann MD, Hagemann M, Forchhammer K. P_{II}-like signaling protein SbtB links cAMP sensing with cyanobacterial inorganic carbon response. Proc Natl Acad Sci USA. 2018; 115(21):E4861-E4869. doi: 10.1073/pnas.1803790115.
40. Selim KA, Haffner M, Burkhardt M, Mantovani O, Neumann N, Albrecht R, Seifert R, Krüger L, Stülke J, Hartmann MD, Hagemann M, Forchhammer K. Diurnal metabolic control in cyanobacteria requires perception of second messenger signaling molecule c-di-AMP by the carbon control protein SbtB. Sci Adv. 2021a; 7(50):eabk0568. doi: 10.1126/sciadv.abk0568.
41. Selim KA, Haffner M, Watzer B, Forchhammer K. Tuning the in vitro sensing and signaling properties of cyanobacterial PII protein by mutation of key residues. Sci Rep. 2019; 9(1):18985. doi: 10.1038/s41598-019-55495-y.
42. Selim KA, Lapina T, Forchhammer K, Ermilova E. Interaction of N-acetyl-l-glutamate kinase with the PII signal transducer in the non-photosynthetic alga Polytomella parva: Co-evolution towards a hetero-oligomeric enzyme. FEBS J. 2020; 287(3):465-482. doi: 10.1111/febs.14989.
43. Selim KA, Tremiño L, Marco-Marín C, Alva V, Espinosa J, Contreras A, Hartmann MD, Forchhammer K, Rubio V. Functional and structural characterization of PII-like protein CutA does not support involvement in heavy metal tolerance and hints at a small-molecule carrying/signaling role. FEBS J. 2021b; 288(4):1142-1162. doi: 10.1111/febs.15464.
44. Shyp V, Dubey BN, Böhm R, Hartl J, Nesper J, Vorholt JA, Hiller S, Schirmer T, Jenal U. Reciprocal growth control by competitive binding of nucleotide second messengers to a metabolic switch in Caulobacter crescentus. Nat Microbiol. 2021; 6(1):59-72. doi: 10.1038/s41564-020-00809-4.
45. Stülke J, Krüger L. Cyclic di-AMP Signaling in Bacteria. Annu Rev Microbiol. 2020; 74:159-179. doi: 10.1146/annurev-micro-020518-115943.
46. Sysoeva TA, Bane LB, Xiao DY, Bose B, Chilton SS, Gaudet R, Burton BM. Structural characterization of the late competence protein ComFB from Bacillus subtilis. Biosci Rep. 2015 Mar 31;35(2):e00183. doi: 10.1042/BSR20140174.
47. Taton A, Erikson C, Yang Y, Rubin BE, Rifkin SA, Golden JW, Golden SS. The circadian clock and darkness control natural competence in cyanobacteria. Nat Commun. 2020; 11(1):1688. doi: 10.1038/s41467-020-15384-9.
48. Walter J, Selim KA, Leganés F, Fernández-Piñas F, Vothknecht UC, Forchhammer K, Aro EM, Gollan PJ. A novel Ca^{2+}-binding protein influences photosynthetic electron transport in Anabaena sp. PCC 7120. Biochim Biophys Acta Bioenerg. 2019; 1860(6):519-532. doi: 10.1016/j.bbabio.2019.04.007.
49. Werel L, Farmani N, Krol E, Serrania J, Essen LO, Becker A. Structural Basis of Dual Specificity of Sinorhizobium meliloti Clr, a cAMP and cGMP Receptor Protein. mBio. 2023; 14(2):e0302822. doi: 10.1128/mbio.03028-22.
50. Yin W, Cai X, Ma H, Zhu L, Zhang Y, Chou SH, Galperin MY, He J. A decade of research on the second messenger c-di-AMP. FEMS Microbiol Rev. 2020; 44(6):701-724. doi: 10.1093/femsre/fuaa019.
51. Yoon SH, Waters CM. The ever-expanding world of bacterial cyclic oligonucleotide second messengers. Curr Opin Microbiol. 2021; 60:96-103. doi: 10.1016/j.mib.2021.01.017.
52. Yoshihara S, Geng X, Okamoto S, Yura K, Murata T, Go M, Ohmori M, Ikeuchi M. Mutational analysis of genes involved in pilus structure, motility and transformation competency in the unicellular motile cyanobacterium Synechocystis sp. PCC 6803. Plant Cell Physiol. 2001; 42(1):63-73. doi: 10.1093/pcp/pce007.
53. Zarrella TM, Yang J, Metzger DW, Bai G. Bacterial Second Messenger Cyclic di-AMP Modulates the Competence State in Streptococcus pneumoniae. J Bacteriol. 2020; 202(4):e00691-19. doi: 10.1128/JB.00691-19.
54. Zeng X, Huang M, Sun QX, Peng YJ, Xu X, Tang YB, Zhang JY, Yang Y, Zhang CC. A c-di-GMP binding effector controls cell size in a cyanobacterium. Proc Natl Acad Sci USA. 2023; 120(13):e2221874120. doi: 10.1073/pnas.2221874120.

Figure 1

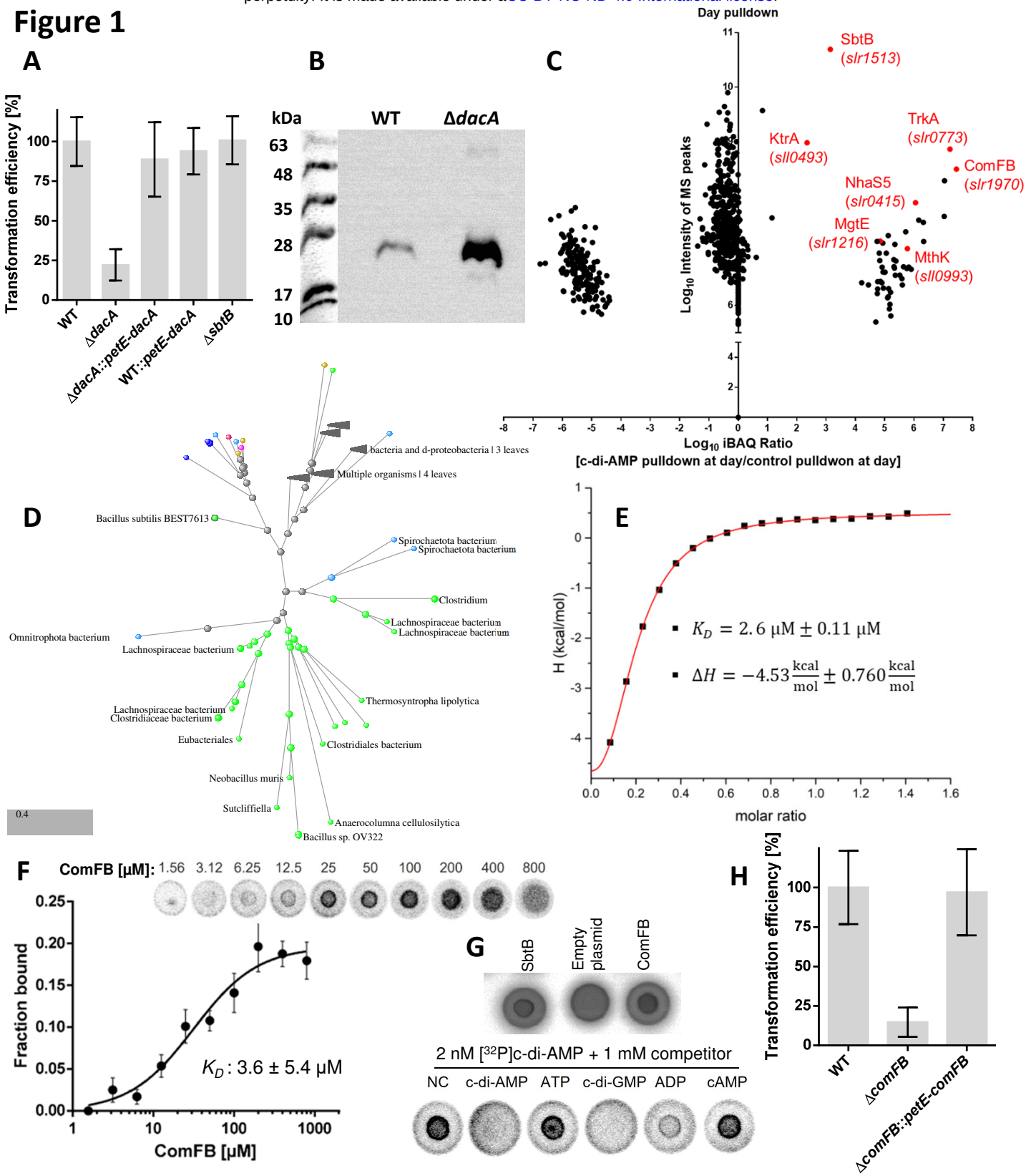

Figure 1. Involvement of c-di-AMP in cyanobacterial natural competence via ComFB signaling protein. (A) Transformation efficiency of WT, Δ*dacA*, *dacA::petE-dacA,* WT*::petE-dacA* and Δ*sbtB* strains. **(B)** Immunodetection of PilA1 in the exoproteome of WT and Δ*dacA*. **(C)** Pulldown experiment using immobilized c-di-AMP and extracts of *Synechocystis* cells grown under day-night cycles, showing the enriched proteins under the day phase. **(D)** Phylogenetic tree showing the widespread of ComFB among different bacterial phyla (detailed tree see Fig. S4). **(E)** Dissociation constant (K_D) of c-di-AMP binding to ComFB and enthalpy (ΔH) are obtained from sigmoidal fitting curve of all ITC experiments with different monomeric ComFB concentrations (60, 72, 134 and 172 μM). **(F)** DRaCALA assay showing the binding of [^{32}P]c-di-AMP to purified ComFB in a concentration dependent manner as indicated. The upper panel shows a representative of one replicate from four technical replicates. The lower panel shows the calculated mean ± SD of the quantification of the bound fraction of [^{32}P]c-di-AMP to ComFB from the four replicates and the best fitting curve with the obtained K_D value. **(G)** DRaCALA competition binding assay showing the competition of [^{32}P]c-di-AMP with different nucleotides to bind ComFB. NC refers to no competitor. SbtB and cell extract of *E. coli* harboring an empty plasmid were used as positive and negative control, respectively. **(H)** Transformation efficiency of WT, Δ*comFB*, and *comFB:*:petE-*comFB* strains.

Figure S1

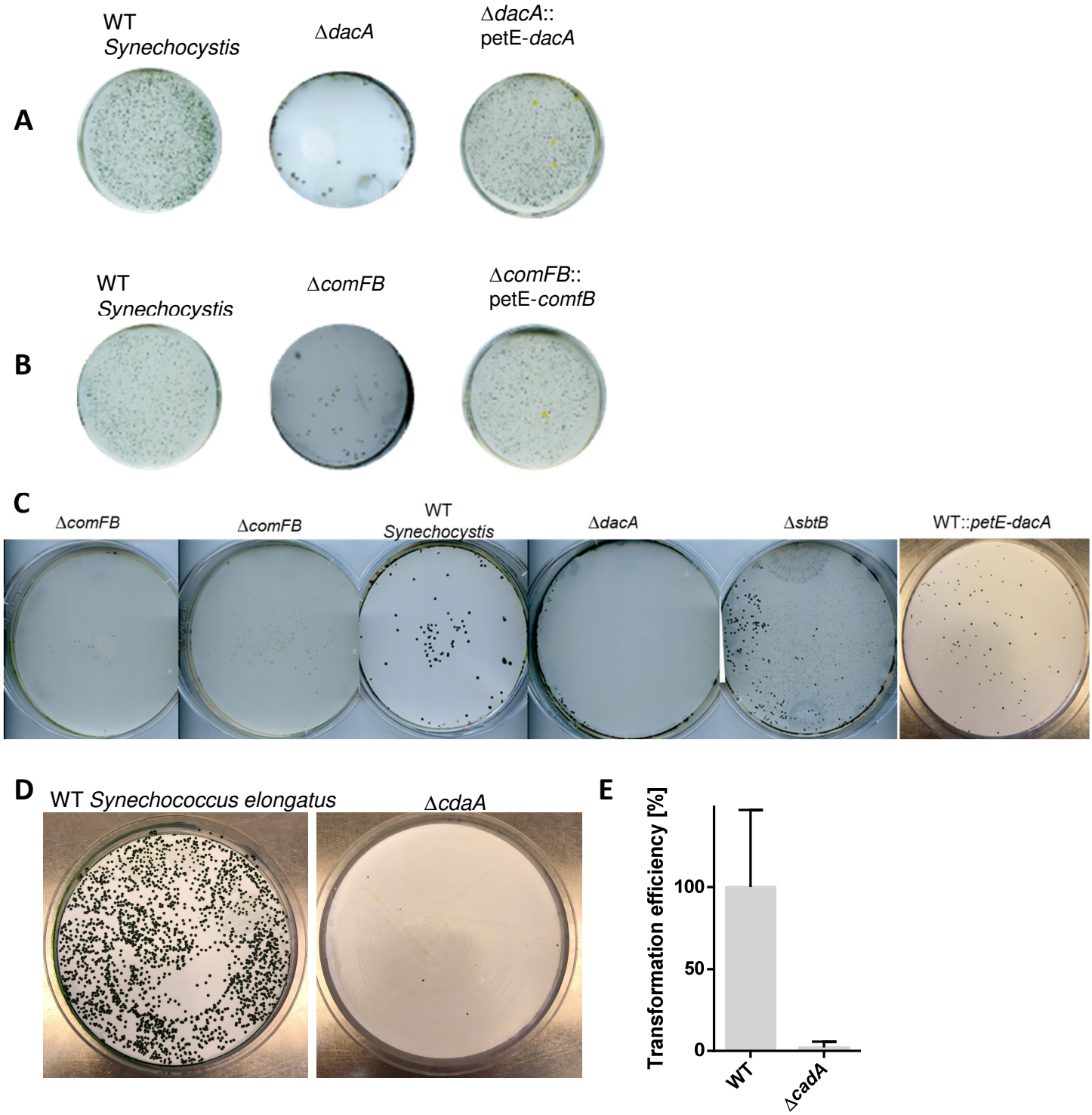

Fig. S1: (A-C) Representative of transformation efficiency in colony forming unites of *Synechocystis* WT, Δ*dacA*, *dacA*::petE-*dacA*, Δ*comFB*, and *comFB*::petE-*comFB* strains using different plasmids with chloramphenicol resistance cassette. Δ*sbtB* mutant was used as a control as another c-di-AMP receptor protein. (D) Representative of transformation efficiency in colony forming unites of *Synechococcus elongatus* WT and Δ*cdaA* mutant. (E) Transformation efficiency of *Synechococcus elongatus* WT and Δ*cdaA* strains.

Figure S2

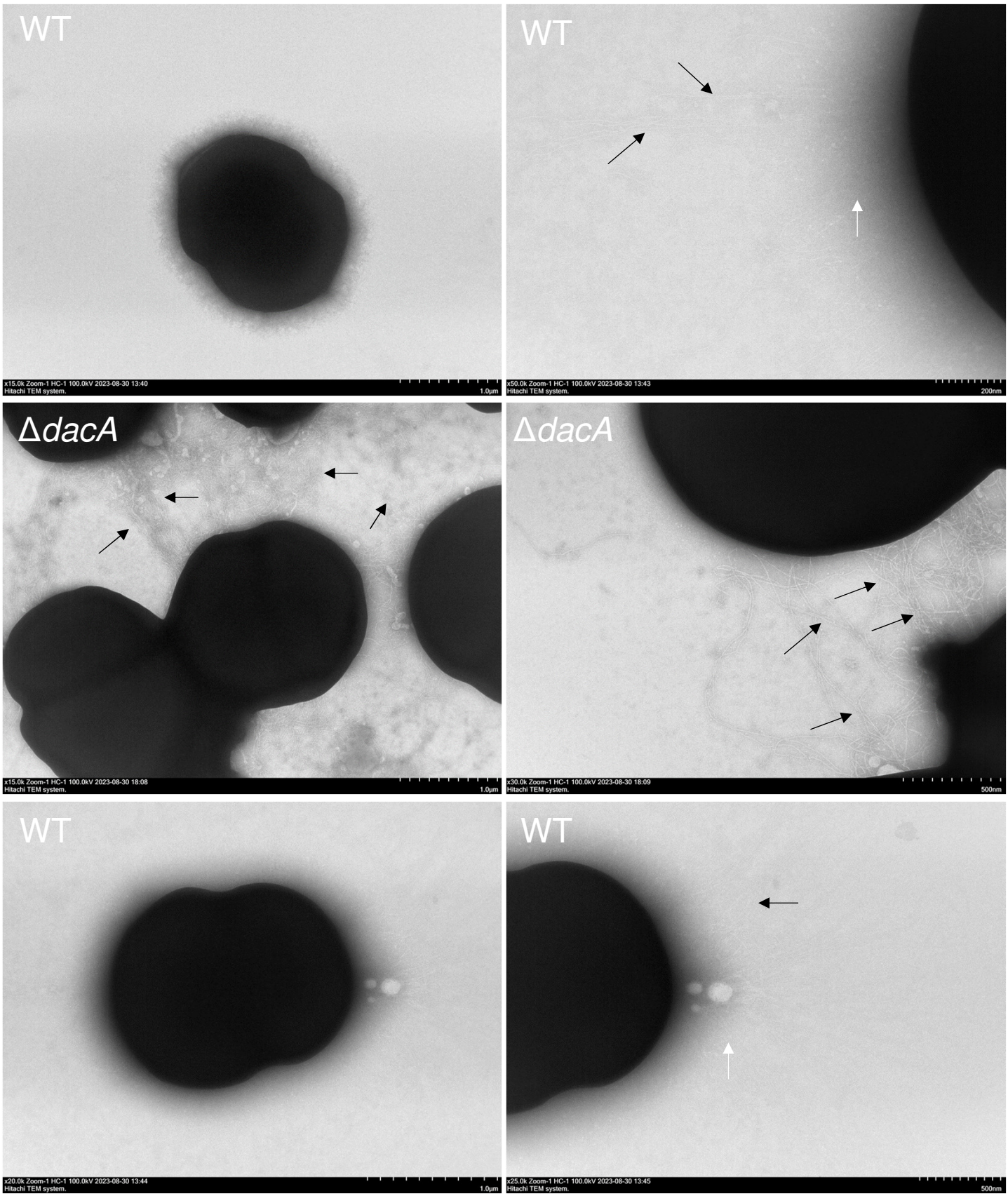

Fig. S2: Electron micrographs of different negatively stained *Synechocystis* and Δ*dacA* mutant, as indicated strains. Whole cells are depicted with 1 µm scale bar and ultrastructural details of pili are shown in 200-500 nm with distinct types of thick pili (black arrow) and thin pili (white arrow).

Figure S3

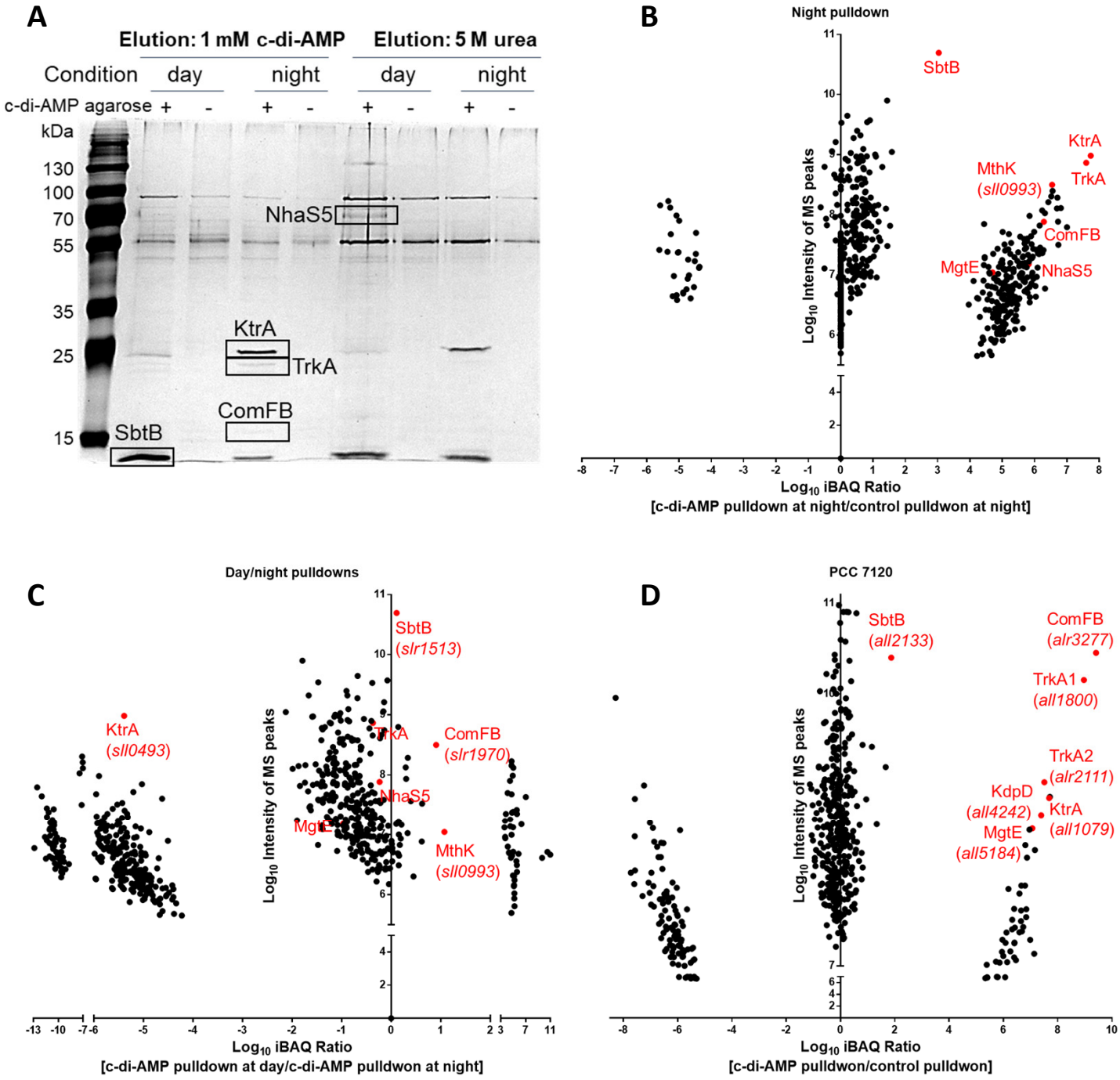

Fig. S3: Identification of potential c-di-AMP binding proteins in *Synechocystis* sp. PCC 6803 and *Nostoc* sp. PCC 7120 using immobilized c-di-AMP pulldowns and analyzed by MS-proteomics. (A) SDS-PAGE of c-di-AMP pulldown elution fractions in *Synechocystis* sp. PCC 6803 under day and night conditions, as indicated, with highlight of the potential targets. Elution of bound proteins was achieved by using 1 mM c-di-AMP or 5 mM urea. (B) Identification of potential c-di-AMP binding proteins in *Synechocystis* sp. PCC 6803 under night, enriched proteins are highlighted in red. (C) enrichment of ComFB in day pulldown compared to night pulldown. (D) Identification of potential c-di-AMP binding proteins in *Nostoc* sp. PCC 7120, enriched proteins are highlighted in red. (B-D) Eluates were analyzed by high accuracy LC-MS/MS to calculate protein enrichment ratios. The identified proteins were sorted by score and refined manually to remove unspecific binning proteins. Significantly enriched proteins were calculated based on Log10 of iBAQ ratio and plotted against the intensity of MS peaks of the identified/defined peptides. The known c-di-AMP receptors: SbtB, TrkA, MgtE and KtrC validated our pulldown approach in general.

Figure S4

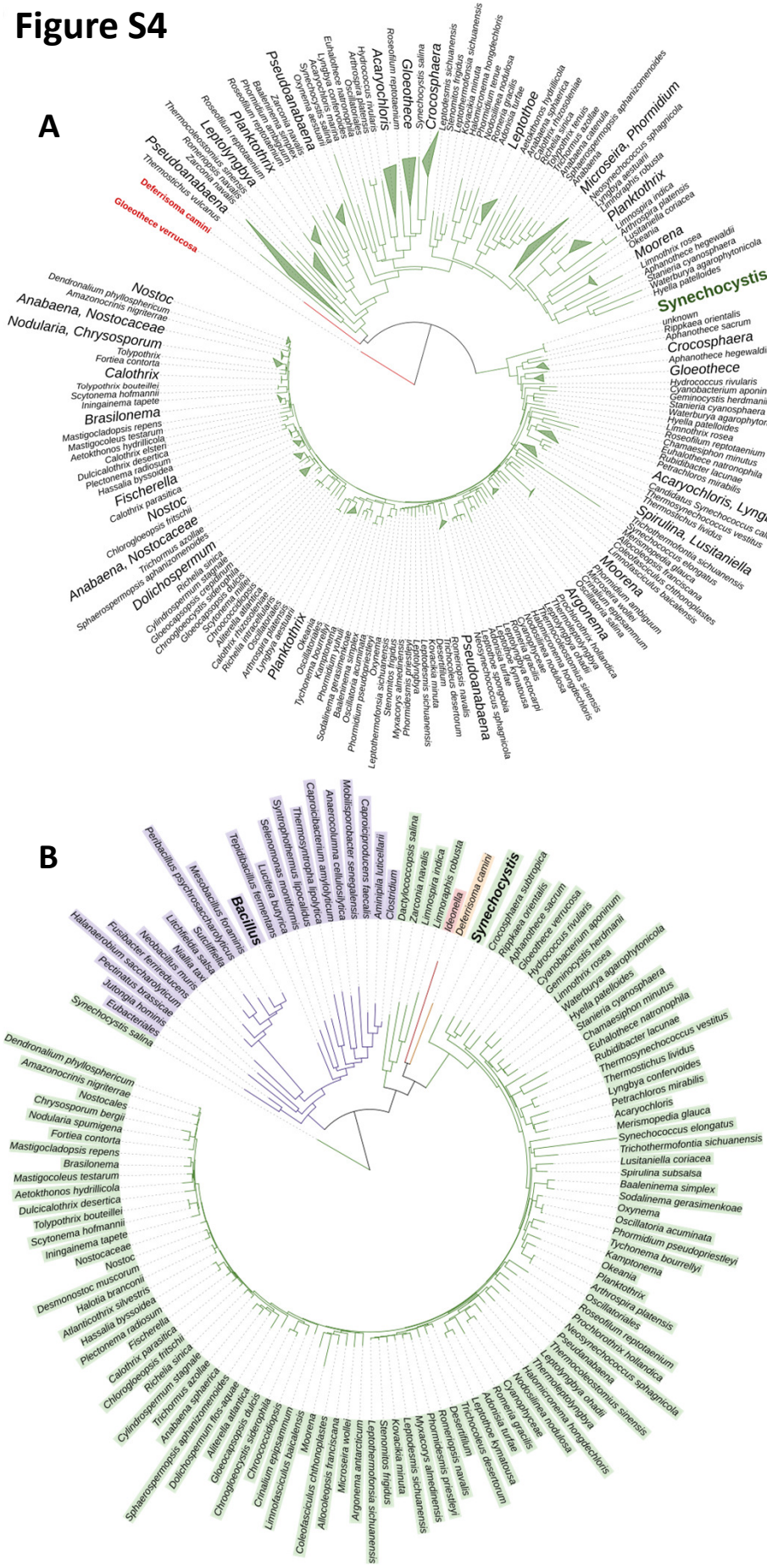

Fig. S4: Rooted phylogenetic tree of ComFB homologs. (A) Distribution among cyanobacteria (green). Collapsed clades are shown as triangles. (B) Distribution among cyanobacteria (green), firmicutes (violet), b-proteobacteria (red) as well as other bacteria (orange). Branch lengths represent genetic divergence. Constructed based on a multiple sequence alignment with sequences obtained from a blastp search of the ComFB domain of Slr1970.

Figure S5

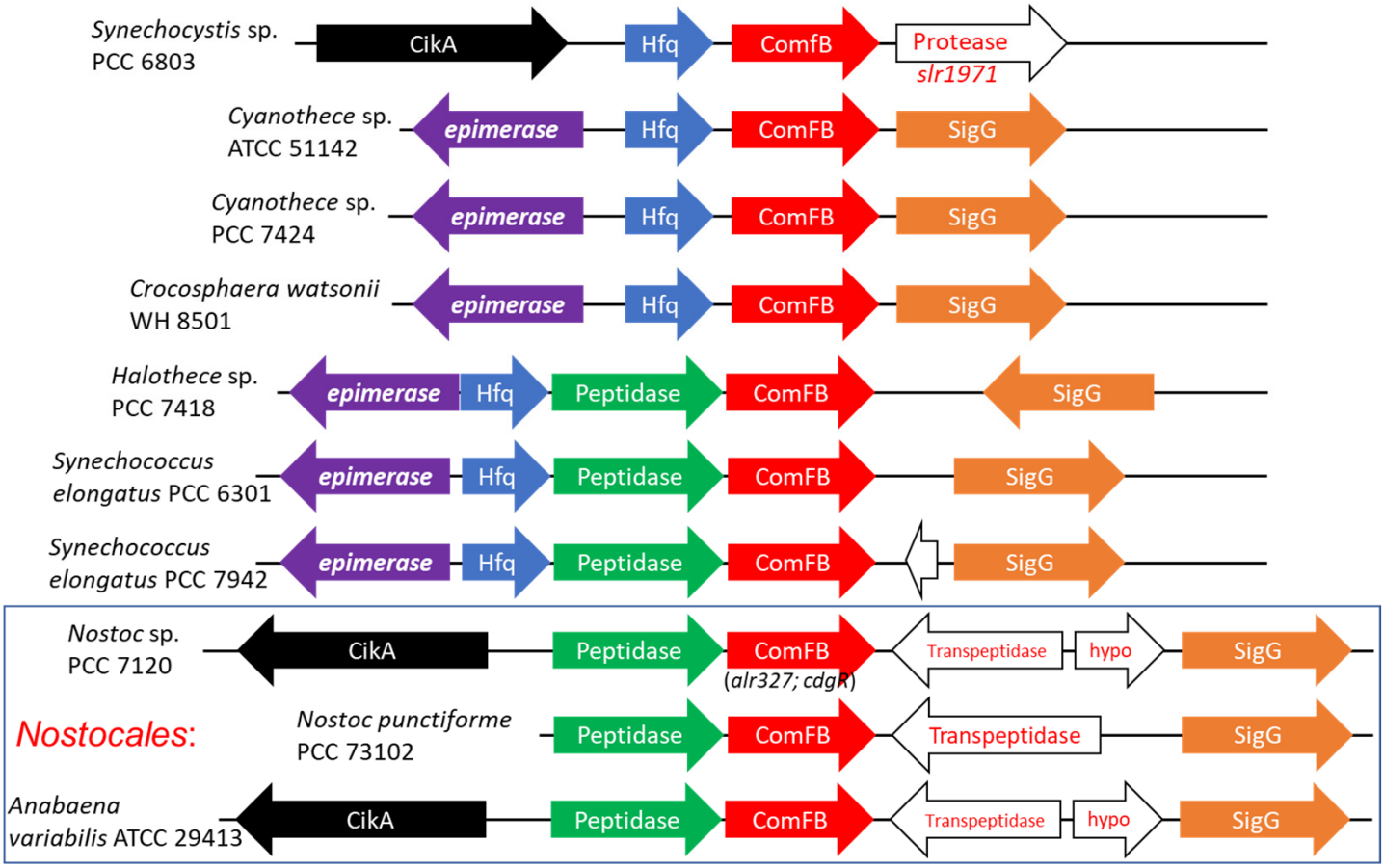

Fig. S5: Genomic organisation and conservation of *comFB* homologs (in red) using SEED database in different cyanobacteria species, as indicated. In *Synechocystis* sp. PCC 6803, upstream of *comfB* (*slr1970*; in red) the open reading frames of *hfq* (*ssr3341*; in blue) and *cikA* (*slr1969;* in black) are found. In other cyanobacterial species, the ORFs (open reading frames) encoding for the RNA polymerase sigma factor (SigG; in orange), putative peptidase (in green) and diaminopimelate epimerase (in violet) are found in association with *comfB* as well. Further ORFs which show no strong conservation (e.g. L,D-transpeptidase) or of hypothetical proteins (hypo) are coloured white.

The ORF coding for an orthologue of the RNA chaperone Hfq (*ssr3341*) is found to be conserved upstream of ComFB homologs in the unicellular cyanobacterial species, while it seems absent from the multicellular filamentous cyanobacteria of order *Nostocales*. Hfq protein is essential for phototaxis and natural competence, which depends on type IV pili (Dienst et al. 2008). Hfq regulates these processes by binding to the PilB1 ATPase subunit of pili machinery (Schuergers et al. 2014). Another conserved ORF found in association with *comFB* is CikA (*slr1969;* circadian input kinase A), encoding for a photoreceptor regulator of the circadian clock in cyanobacteria (Cohen & Golden 2015; Narikawa et al. 2008). The sigma factors are also involved in circadian clock regulation (Nair et al. 2002). Since ComFB is found in genomic organization with Hfq and circadian clock components, it seems logical that these proteins are also related in their function. Therefore, this further implies the involvement of ComFB in the regulation of light-dependent processes like natural competence or phototaxis (Taton et al. 2020; Menon et al. 2021), which are type IV pili dependent processes.

Figure S6

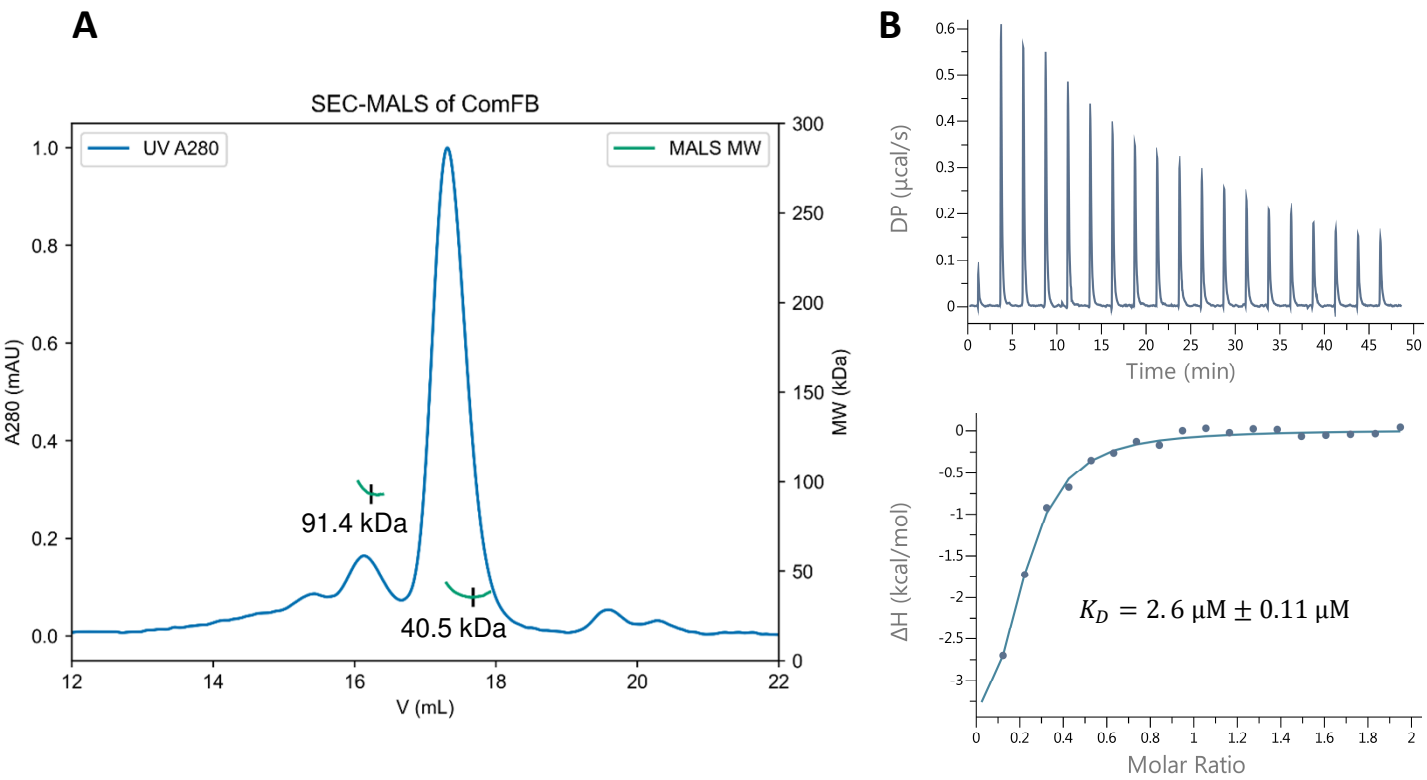

Fig. S6: Characterization of ComFB protein encoded by *slr1970*. (A) Size exclusion chromatography coupled to multiangle light scattering (SEC-MALS) of recombinantly purified ComFB. Absorption at 280 nm (A280) is plotted against elution volume (V) from a Superose 6 Increase 10/300 GL column. Molecular weight (MW) obtained from MALS is plotted for the two main peaks in the A280 signal, with minima in the MW marked. The major peak of ComFB (thermotical mass of monomer 20.6 kDa) showed a ~ 40.5 kDa molar mass, indicating that ComFB behaves as a dimmer in solution, however a small fraction of the protein behaved as a tetramer as indicated by 91. kDa molar mass. (B) Representative isothermal titration calorimetry (ITC) measurements of 172 µM ComFB (monomeric concentration) titrated with 1 mM c-di-AMP. Upper panel shows the recorded differential power (DP) signal of ligand-to-protein titration, plotted against time. The enthalpy changes for each injected (ΔH) are calculated by subtraction of a differential power signal from buffer-in-protein titration control, and subsequent integration of the DP peaks, and plotted against molar ratio of ligand to protein. Lower panel shows the binding isotherms and the best-fit curves according to the one-set of binding sites for dimeric ComFB with K_D of 2.6 ± 0.11 µM.

Figure S7

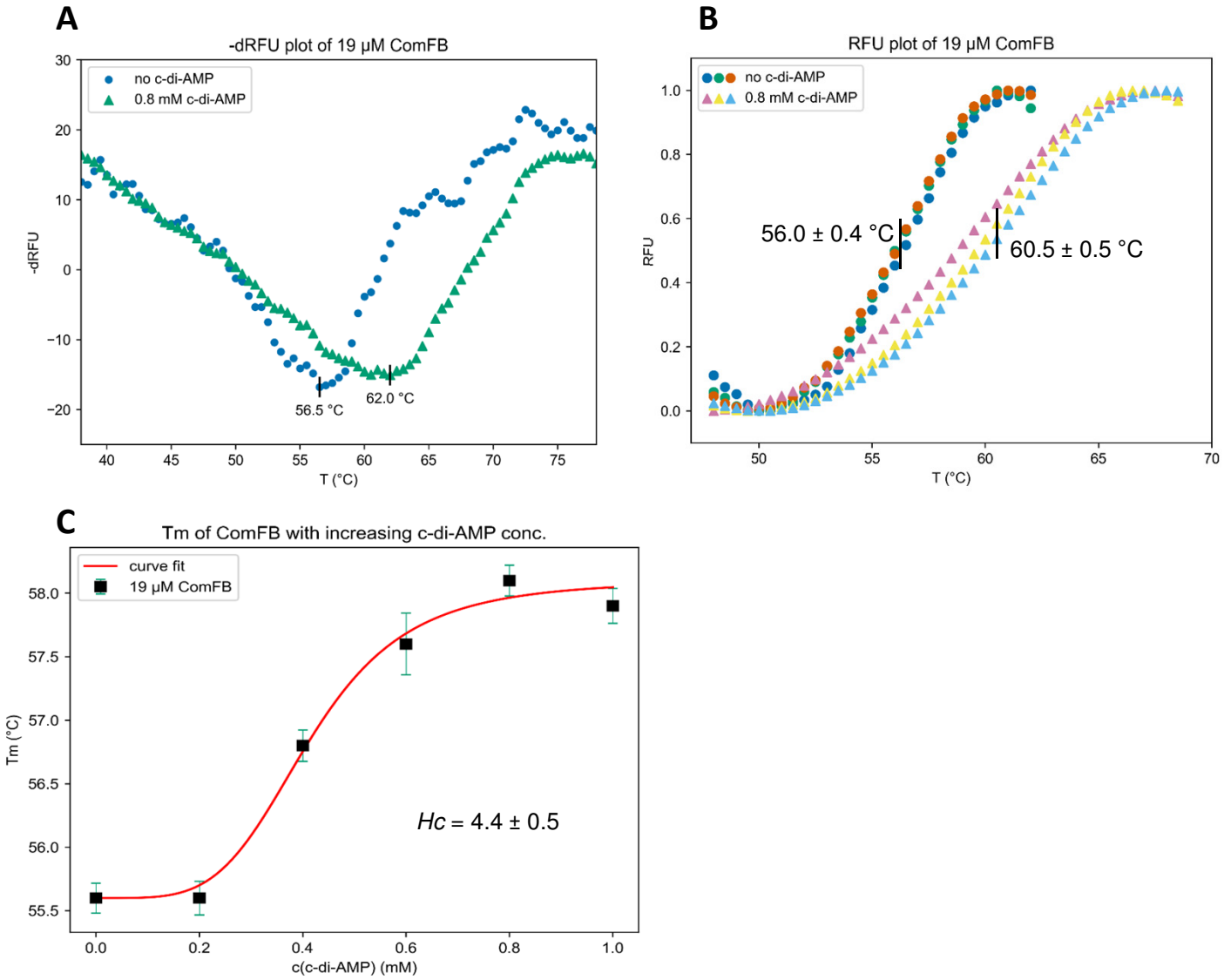

Fig. S7: Thermal shift assay showing binding of c-di-AMP to ComFB. (A) Negative first derivative of representative ComFB (19 µM) melting profiles with and without c-di-AMP (0.8 mM), calculated from thermal shift assay data. Minima in the calculated negative first derivative of recorded relative fluorescence units (-dRFU) over temperature (T) represent the melting temperatures of the protein. (B) Melting profile of 19 µM ComFB with and without 0.8 mM c-di-AMP, recorded in a thermal shift assay. The fluorescence emission of SYPRO Orange at 570 nm was followed over a temperature range of 25-99 °C, and normalised relative fluorescence units (RFU) were plotted against temperature (T). Temperatures at half-maximal normalised fluorescence emission are indicated. Measurements were performed in triplicates. (C) Melting temperatures (Tm) of 19 µM ComFB in the presence of different concentrations of c-di-AMP; Melting temperatures were calculated from -dRFU/dT plots as in (A). Measurements were performed in triplicates, error bars show the standard deviation from the calculated mean melting temperature. The data were fitted with the Hill equation. Hill coefficient (*Hc*) is in positive value, indicative of cooperativity between binding sites. Calculated values of the fitting parameters and their variance are indicated.

Figure S8

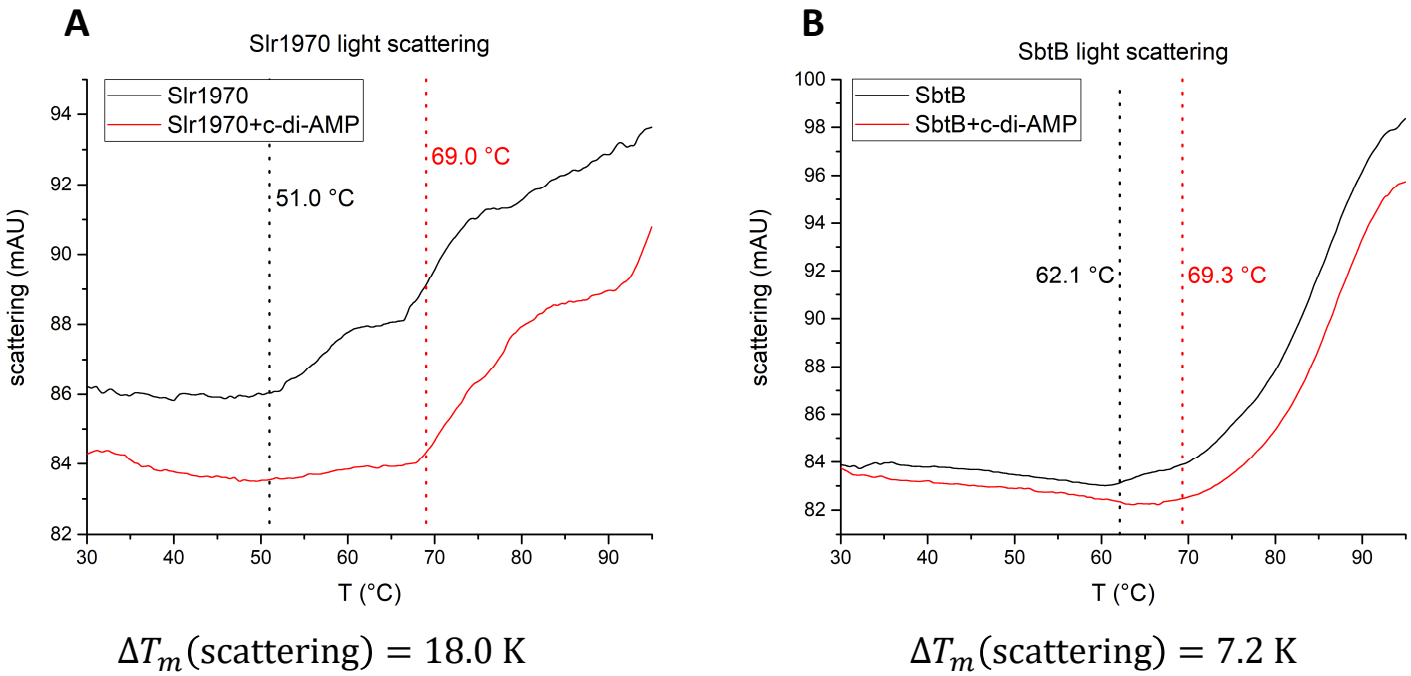

$\Delta T_m(\text{scattering}) = 18.0\ \text{K}$

$\Delta T_m(\text{scattering}) = 7.2\ \text{K}$

Fig. S8: Light scattering obtained from the thermal shift assay using nanoDSF. The calculated temperatures from which the light scattering increases are shown as indicated. The temperature shift (ΔT_m) between proteins (1.5 mg/ml) with and without c-di-AMP (0.5 mM) is shown as indicated. (A) Light scattering of ComFB (Slr1970), while (B) light scattering of SbtB (used as +ve control as known c-di-AMP receptor protein) (Selim et al. 2021).

Figure S9

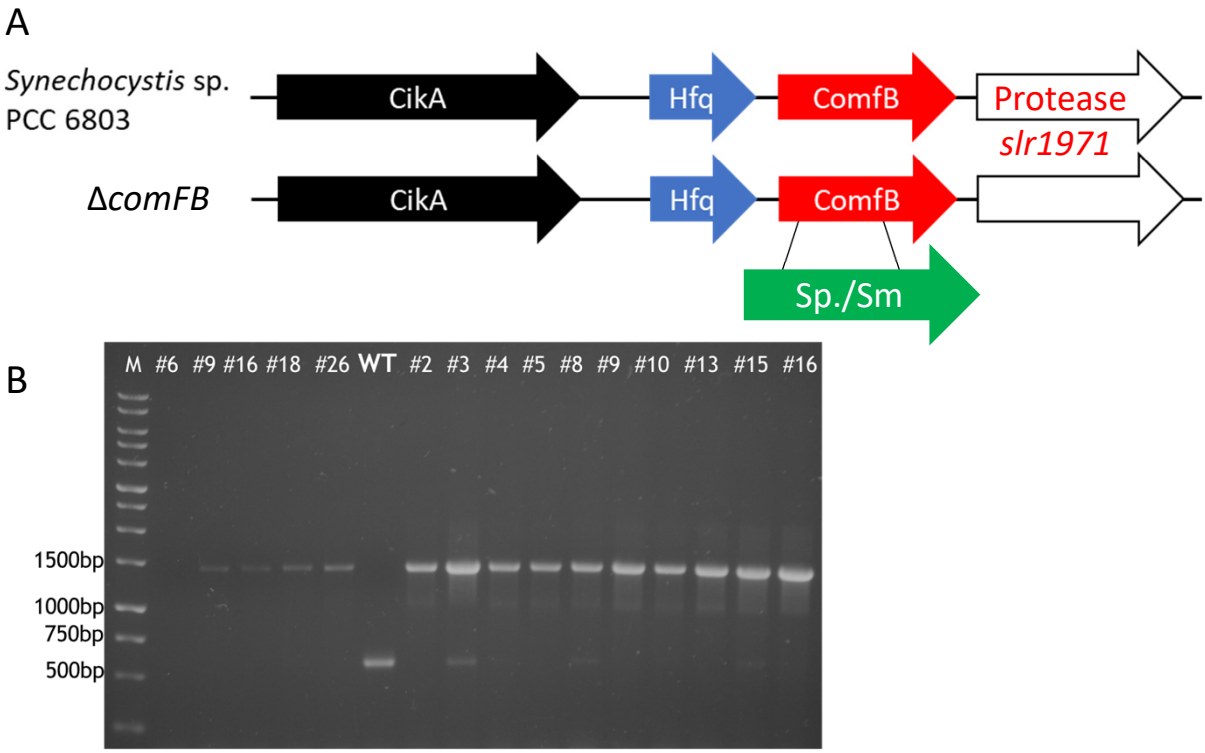

Fig. S9: Genotypic characterization of Δ*comFB* knockout mutant. (A) Schematic representation of genetic organization of *slr1970* (designated *comFB*) gene in the *Synechocystis* sp. PCC 6803 genome, the deletions of the gene by replacement with spectinomycin/streptomycin (Sp./Sm.) resistance cassette. (B) PCR showing complete segregation of Sp./Sm-resistance-cassette Δ*comFB* knockout from independent colonies (#6, #9, ….. etc). The PCR product for the wildtype (WT) and the Δ*comF*B knockout is 600 bp and around 1450 bp, respectively.

Figure S10

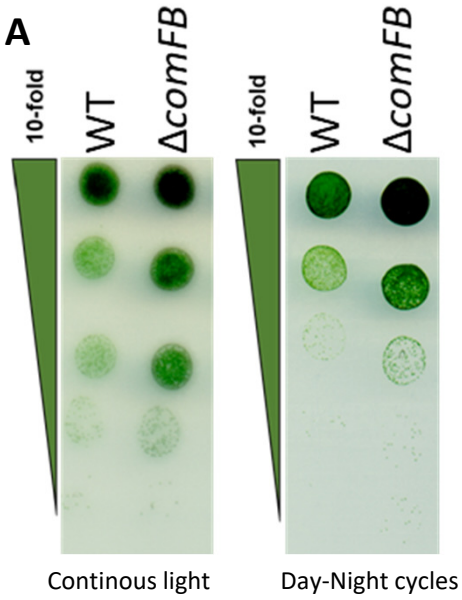

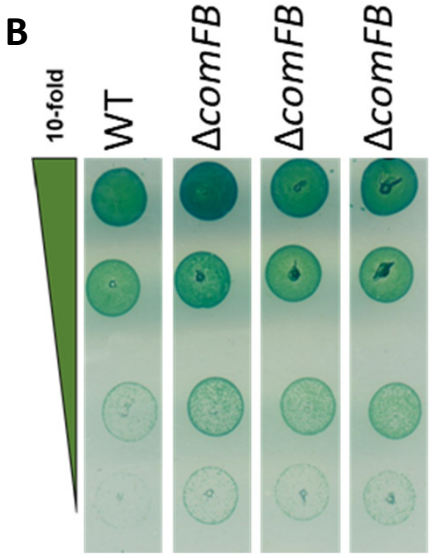

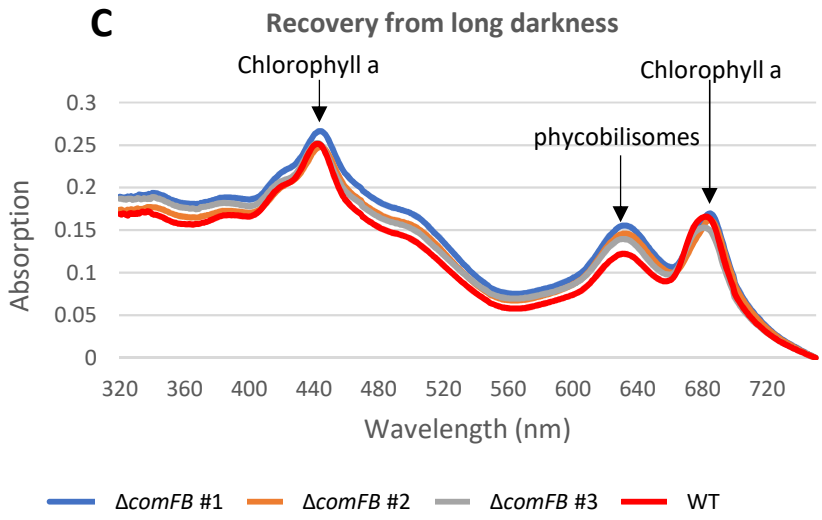

Fig. S10: Phenotypic characterization of Δ*comFB* under different light conditions. (A) Growth test by drop plate assay of *Synechocystis* WT and Δ*comFB* cells under either continuous light (left) or a 12-hour diurnal rhythm (right). (B) Viability test using the drop-plate assay of *Synechocystis* WT and Δ*comFB* (3 independent clones of the mutant) cells after 6 days of incubation in complete darkness. Cells were normalized to an optical density at 750 nm (OD_{750}) of 1.0 and serial diluted in 10-fold steps (top to bottom; depicted by a green triangle). (C) Whole cell spectra of *Synechocystis* WT cells in comparison to Δ*comFB* cells after 2 days of recovery from darkness (6 days). The peak representing phycobilisomes as well as the peaks representing chlorophyll a are depicted by black arrows. Cultures were normalized to similar OD_{750}.

Figure S11

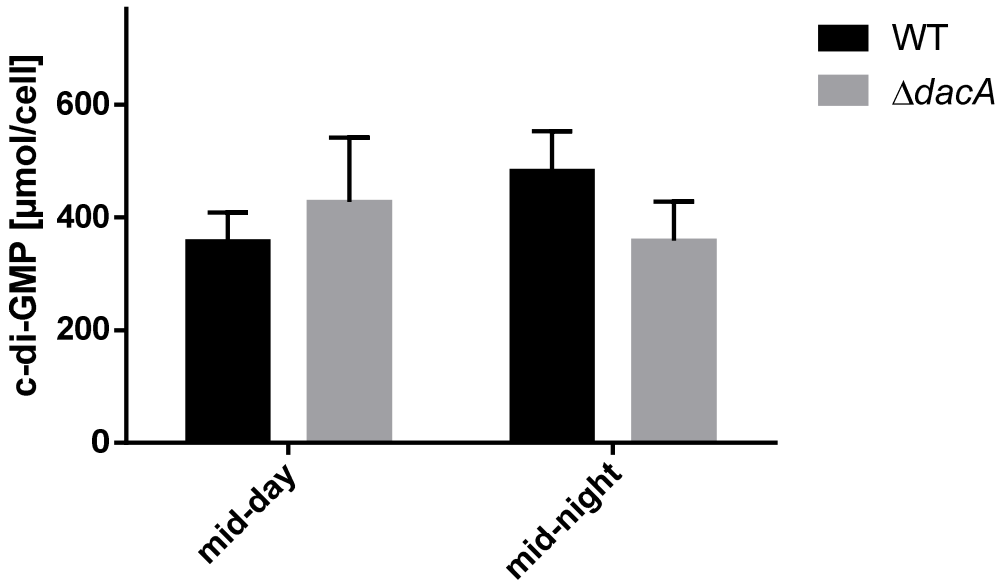

Fig. S11: c-di-GMP concentration throughout a 12 h diurnal rhythm within *Synechocystis* WT (black bars) and ΔdacA cells (gray bars) at either mid of day or night phase (i.e. 6 h of light or darkness). X-axis shows the time in hours; Y-axis shows the intracellular concentrations of c-di-GMP.

Figure S12

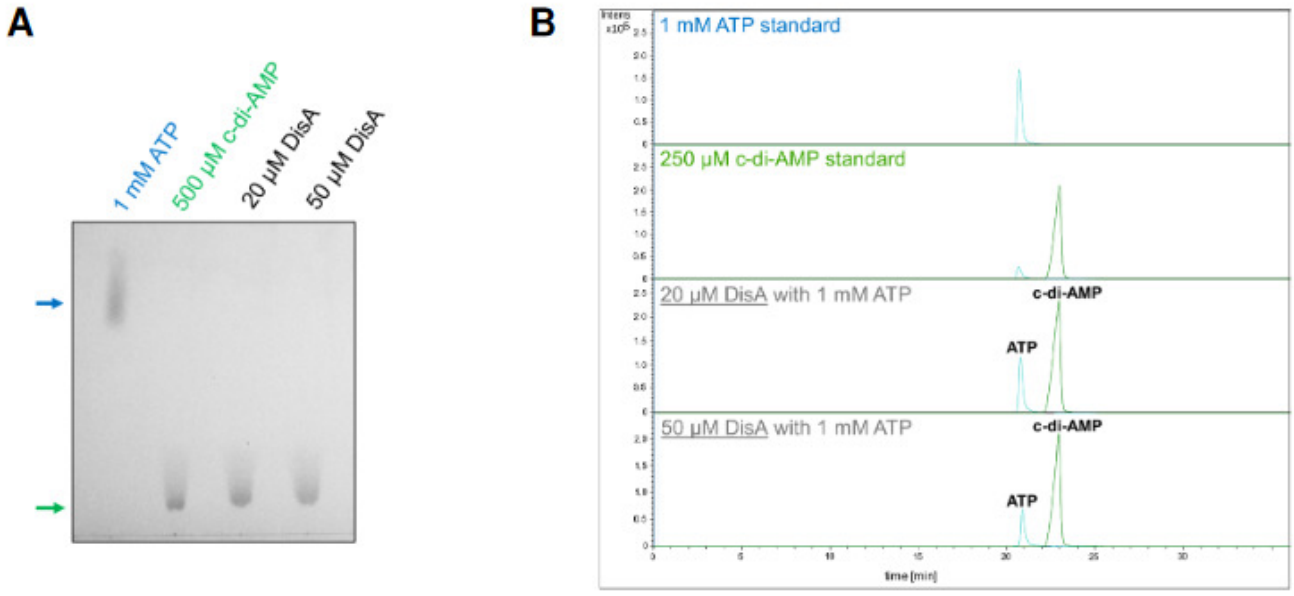

Fig. S12: Synthesis of c-di-AMP from purified DisA. Analysis of the enzymatic conversion of 1 mM ATP to c-di-AMP with 20 µM or 50 µM recombinant DisA. (A) Thin layer chromatography (TLC). Arrows denote running distance of c-di-AMP (green) and ATP (blue). (B) LC-MS analysis of purified His_6-tagged DisA showing conversion of ATP to c-di-AMP.

Supporting materials references:

- Cohen SE, Golden SS. Circadian Rhythms in Cyanobacteria. Microbiol Mol Biol Rev. 2015; 79(4):373-85. doi: 10.1128/MMBR.00036-15.
- Dienst D, Dühring U, Mollenkopf HJ, Vogel J, Golecki J, Hess WR, Wilde A. The cyanobacterial homologue of the RNA chaperone Hfq is essential for motility of Synechocystis sp. PCC 6803. Microbiology (Reading). 2008; 154(Pt 10):3134-3143. doi: 10.1099/mic.0.2008/020222-0.
- Menon SN, Varuni P, Bunbury F, Bhaya D, Menon GI. Phototaxis in Cyanobacteria: From Mutants to Models of Collective Behavior. mBio. 2021; 12(6):e0239821. doi: 10.1128/mBio.02398-21.
- Nair U, Ditty JL, Min H, Golden SS. Roles for sigma factors in global circadian regulation of the cyanobacterial genome. J Bacteriol. 2002; 184(13):3530-8. doi: 10.1128/JB.184.13.3530-3538.2002.
- Narikawa R, Kohchi T, Ikeuchi M. Characterization of the photoactive GAF domain of the CikA homolog (SyCikA, Slr1969) of the cyanobacterium Synechocystis sp. PCC 6803. Photochem Photobiol Sci. 2008; 7(10):1253-9. doi: 10.1039/b811214b.
- Schuergers N, Ruppert U, Watanabe S, Nürnberg DJ, Lochnit G, Dienst D, Mullineaux CW, Wilde A. Binding of the RNA chaperone Hfq to the type IV pilus base is crucial for its function in Synechocystis sp. PCC 6803. Mol Microbiol. 2014; 92(4):840-52. doi: 10.1111/mmi.12595.
- Selim KA, Haffner M, Burkhardt M, Mantovani O, Neumann N, Albrecht R, Seifert R, Krüger L, Stülke J, Hartmann MD, Hagemann M, Forchhammer K. Diurnal metabolic control in cyanobacteria requires perception of second messenger signaling molecule c-di-AMP by the carbon control protein SbtB. Sci Adv. 2021; 7(50):eabk0568. doi: 10.1126/sciadv.abk0568.
- Taton A, Erikson C, Yang Y, Rubin BE, Rifkin SA, Golden JW, Golden SS. The circadian clock and darkness control natural competence in cyanobacteria. Nat Commun. 2020; 11(1):1688. doi: 10.1038/s41467-020-15384-9.